

Effects of conservation of total angular momentum on two-hard-particle systems

Masayuki Uranagase*

Department of Applied Mathematics and Physics, Graduate School of Informatics, Kyoto University, Kyoto 606-8501, Japan

(Received 27 July 2007; revised manuscript received 22 October 2007; published 10 December 2007)

In this paper we investigate some statistical mechanical properties of systems consisting of two hard disks in a circular cavity and two hard spheres in a cylindrical pore. Both systems conserve not only the total energy but the total angular momentum, and this conservation affects thermodynamic quantities such as the temperature and pressure of these systems. We show the dependence of the thermodynamic quantities of these systems on conserved quantities with a statistical mechanical treatment and molecular dynamics simulations.

DOI: [10.1103/PhysRevE.76.061111](https://doi.org/10.1103/PhysRevE.76.061111)

PACS number(s): 05.20.-y, 05.20.Gg, 05.45.Ac

I. INTRODUCTION

Investigations of systems confined to a vessel or a slit are important for the understanding of the behavior of nanosystems and have already been done extensively [1,2]. Confinement of substances in a vessel changes some properties from those of the bulk, e.g., the freezing temperature of porous systems shifts from that of the bulk systems [1]. To explain experimental results and predict new properties of confined systems, many researchers have studied these systems with various interaction potentials not only (numerical) experimentally but also theoretically.

A system consisting of particles with a hard core potential is one of the simplest models. In spite of the simplicity of a hard sphere model, it yields interesting and nontrivial behavior. Confined hard disk or sphere systems have been investigated from the viewpoint of statistical mechanics [3–8] and dynamical systems [9,10]. Freezing and glass transitions of hard disk systems in a circular cavity have been investigated by molecular dynamics simulations [3,4]. Román *et al.* computed the density profiles [5] and velocity distribution [6] of this system, taking into account the effect of the conservation of the total angular momentum. A system of hard spheres in a cylindrical pore exhibits interesting properties associated with a phase transition. For instance, the structure of this system experiences transitions when the radius of the pore is changed at zero temperature [11]. It is also observed that a sudden change in the density occurs when the radius of the pore exceeds some value which is related to the appearance of a van der Waals loop [12].

In this paper, we treat very small systems, i.e., two hard disks in a circular cavity and two hard spheres in a cylindrical pore. In spite of the smallness of the system, it is not easy to understand the statistical mechanical properties of two-particle systems. However, in some cases, one can exactly compute the phase space volumes of two-particle systems [13–16] and they predict unexpected behavior. For instance, the phase space volume of a system consisting of two hard disks or spheres in a rectangular box can be computed exactly, and the compressibility in one direction, which is obtained from the phase space volume, becomes negative for a certain size of the box [13,14]. This behavior is confirmed from molecular dynamics simulations [14,17].

This paper is organized as follows. In Sec. II, we consider the phase space volume of a system consisting of two hard disks in a circular cavity. This system conserves not only its energy but also its total angular momentum, and this conservation complicates analytical computation of the phase space volume. This forces us to do numerical integration at the final stage of the computation of the phase space volume. From this phase space volume, we can compute thermodynamic quantities such as entropy, temperature, and pressure, and we compare these theoretical results with those obtained from molecular dynamics simulations to check the ergodicity of the system numerically. In particular, we focus on the dependence of thermodynamic quantities on the total angular momentum. We also discuss the cause of the large statistical error of the pressure when the size of the cavity is small. After showing results for the two-dimensional system, we study a system consisting of two hard spheres in a cylindrical pore in Sec. III. In this system, calculations of thermodynamic quantities are similar to those of two hard disks in a circular cavity. Here, we pay attention to the behavior of pressure in the longitudinal direction; a negative compressibility region appears when both the absolute value of the total angular momentum and radius of the pore are small. Section IV is a summary.

II. TWO HARD DISKS IN A CIRCULAR CAVITY

Now we consider a circular cavity with a radius R which contains two hard disks, each with a diameter d and mass m . The center of each hard disk can move in a circle whose radius is $R-d/2$. We assume that the hard disk collides with the wall of the circular cavity elastically. For this system, it is useful to express the position and momentum of the i th hard disk ($i=1,2$) as a polar coordinate $\mathbf{q}_i=(r_i, \theta_i)$ and a conjugate momentum $\mathbf{p}_i=(p_{r,i}, p_{\theta,i})$, respectively. Then, the Hamiltonian of this system is given by

$$H_{\text{cir}} = \sum_{i=1}^2 \left(\frac{p_{r,i}^2}{2m} + \frac{p_{\theta,i}^2}{2mr_i^2} + V_{\text{ext}}(\mathbf{q}_i) \right) + V_{\text{int}}(|\mathbf{q}_1 - \mathbf{q}_2|), \quad (1)$$

where $V_{\text{ext}}(\mathbf{q}_i)$ is the potential that confines the i th hard disk in the circular cavity,

$$V_{\text{ext}}(\mathbf{q}_i) = \begin{cases} 0, & 0 \leq r_i \leq R - d/2, \\ \infty & \text{otherwise,} \end{cases} \quad (2)$$

*masayuki@amp.i.kyoto-u.ac.jp

and $V_{\text{int}}(|\mathbf{q}_1 - \mathbf{q}_2|)$ is the interaction potential between two hard disks,

$$V_{\text{int}}(|\mathbf{q}_1 - \mathbf{q}_2|) = \begin{cases} 0, & |\mathbf{q}_1 - \mathbf{q}_2| \geq d, \\ \infty, & |\mathbf{q}_1 - \mathbf{q}_2| < d. \end{cases} \quad (3)$$

In the phase space, the motion of this system is restricted to the surface with constant total angular momentum \mathcal{L} and energy \mathcal{E} . The entropy of this system S is defined by [18–21]

$$S = \ln \Gamma_{\text{cir}}(\mathcal{E}, \mathcal{L}). \quad (4)$$

Here $\Gamma_{\text{cir}}(\mathcal{E}, \mathcal{L})$ is the volume bounded by the energy surface $H = \mathcal{E}$ on the surface $p_{\theta,1} + p_{\theta,2} = \mathcal{L}$ in the phase space, i.e.,

$$\Gamma_{\text{cir}}(\mathcal{E}, \mathcal{L}) = \int \left(\prod_{i=1}^2 dr_i d\theta_i dp_{r,i} dp_{\theta,i} \right) \Theta(\mathcal{E} - H_{\text{cir}}) \times \delta\left(\mathcal{L} - \sum_{i=1}^2 p_{\theta,i}\right), \quad (5)$$

where $\Theta(x)$ and $\delta(x)$ are the Heaviside and Dirac delta function, respectively. This definition of entropy is convenient for this system since the temperature obtained from Eq. (8) below is consistent with the equipartition law (see Fig. 1 below), even if the degree of freedom of the system is small [22]. Performing the integration in Eq. (5) over $p_{r,i}$ and $p_{\theta,i}$ ($i=1,2$) gives the volume of the three-dimensional ellipsoid whose radii are κ , κ , and $r_1 r_2 \kappa / \sqrt{r_1^2 + r_2^2}$, where $\kappa = \sqrt{2m\mathcal{E} - \mathcal{L}^2 / (r_1^2 + r_2^2)}$. In addition, we integrate Eq. (5) over θ_1 and θ_2 to obtain

$$g(r_1, r_2; d) = \begin{cases} 0, & \frac{r_1^2 + r_2^2 - d^2}{2r_1 r_2} < -1, \\ 4\pi \left[\pi - \cos^{-1} \left(\frac{r_1^2 + r_2^2 - d^2}{2r_1 r_2} \right) \right], & -1 \leq \frac{r_1^2 + r_2^2 - d^2}{2r_1 r_2} \leq 1, \\ 4\pi^2, & \frac{r_1^2 + r_2^2 - d^2}{2r_1 r_2} > 1. \end{cases} \quad (7)$$

The remaining integration in Eq. (6) over r_1 and r_2 is performed numerically to obtain $\Gamma_{\text{cir}}(\mathcal{E}, \mathcal{L})$ explicitly.

The temperature T is obtained from S through the thermodynamic relation as [18,19,23]

$$T = \left(\frac{\partial S}{\partial \mathcal{E}} \right)^{-1}. \quad (8)$$

In this paper, as units of length and mass we choose the diameter d and the mass m of a hard disk, respectively. The unit of time is chosen so that the Boltzmann constant $k_B = 1$. We take $\mathcal{E} = 3/2$ for this system. In Fig. 1, we show the dependence of T on \mathcal{L} for the cases $R=2$ and 2.5. Here we also

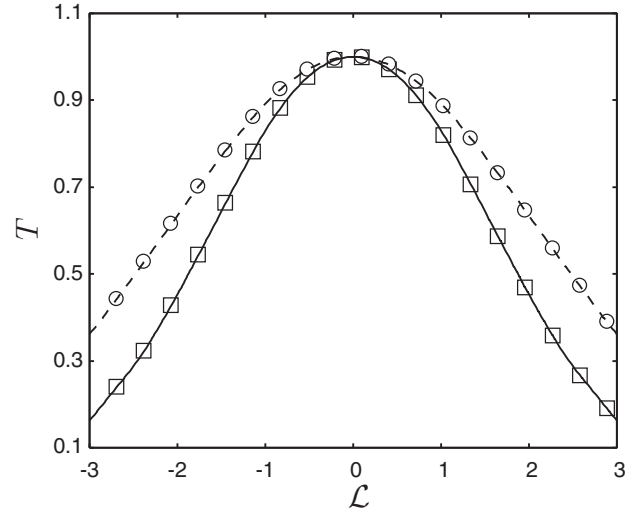


FIG. 1. Dependence of T on \mathcal{L} for the system with two hard disks in circular cavities with different R . Curves were obtained from Eq. (8) for $R=2$ (solid) and 2.5 (dashed). Points represent long-time average of $p_{r,1}^2/m$ obtained from molecular dynamics simulations for $R=2$ (squares) and 2.5 (circles). We set $\mathcal{E}=3/2$ in both cases.

$$\Gamma_{\text{cir}}(\mathcal{E}, \mathcal{L}) = \int_0^{R-d/2} dr_1 \int_0^{R-d/2} dr_2 \frac{4\pi r_1 r_2}{3(r_1^2 + r_2^2)^2} [2m\mathcal{E}(r_1^2 + r_2^2) - \mathcal{L}^2]^{3/2} g(r_1, r_2; d) \Theta(2m\mathcal{E}(r_1^2 + r_2^2) - \mathcal{L}^2), \quad (6)$$

where $g(r_1, r_2; d)$, in which the d dependency is explicitly written for later convenience, is

plot the long-time average of $p_{r,1}^2/m$, $\langle p_{r,1}^2/m \rangle$, computed from molecular dynamics simulations, to show that the average of $p_{r,1}^2/(2m)$ is equal to $T/2$ obtained from Eq. (8). Replacing \mathcal{L} in Eq. (6) by $-\mathcal{L}$, we recognize that T is an even function of \mathcal{L} , which is consistent with Fig. 1. It is confirmed from Fig. 1 that T has a maximum value at $\mathcal{L}=0$ and decreases monotonically as the absolute value of \mathcal{L} , $|\mathcal{L}|$, increases. We also see that the temperature for $R=2.5$ is higher than that for $R=2.0$, except for $\mathcal{L}=0$, where the two temperatures coincide. These results are related to the fact that the phase space volume is reduced as \mathcal{L} becomes large and R becomes small. In other words, it is easy for $p_{r,1}^2/(2m)$ to be large when \mathcal{L} is small and/or R is large. It is worth noting

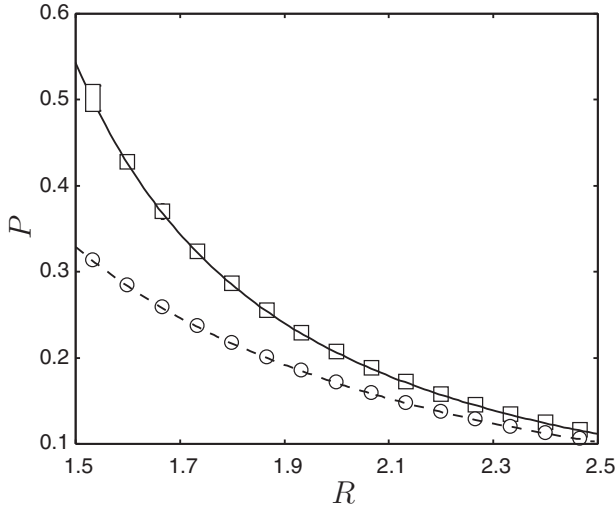


FIG. 2. Pressure as a function of R for the system with two hard disks in circular cavities with different \mathcal{L} . Curves represent the result of Eq. (9) for $\mathcal{L}=0$ (solid) and 2 (dashed). Points represent the result of molecular dynamics simulations for $\mathcal{L}=0$ (squares) and 2 (circles). We set $\mathcal{E}=3/2$.

that Eq. (6) is written as $\Gamma_{\text{cir}}(\mathcal{E}, \mathcal{L}) = \mathcal{E}^{3/2} \times (\text{terms independent of } \mathcal{E})$ when $\mathcal{L}=0$. Hence, when $\mathcal{L}=0$, $T=2\mathcal{E}/3$, which is independent of R .

From the thermodynamic relation, the pressure is given by [23]

$$P = T \left(\frac{\partial S}{\partial V} \right) = \frac{T}{2\pi R} \left(\frac{\partial S}{\partial R} \right), \quad (9)$$

where $V (= \pi R^2)$ signifies the volume of the circular cavity. On the other hand, we can calculate a pressure, which we denote by P_{MD} , from molecular dynamics simulation as a time average,

$$P_{\text{MD}}(\tau) = \frac{1}{\tau} \frac{\sum_{i=1}^2 \sum_{n=1}^{N_i} 2p_{i,r}(n)}{2\pi R}. \quad (10)$$

Here $2p_{i,r}(n)$ is the momentum transfer from the i th hard disk to the wall due to the n th collision, and N_i is the total number of collisions of the i th hard disk with the wall in time τ . Below, we compare the pressure defined by Eq. (9) with that obtained from molecular dynamics simulations.

Figure 2 shows pressure as a function of R for the cases $\mathcal{L}=0$ and 2. In the simulations, we set $\tau=10^5$ in Eq. (10) and performed simulations starting from 1000 different initial conditions for each data point in order to achieve good statistics. It is noted that the statistical error is less than the point size. The pressure decreases monotonically as R increases in both cases, and we do not observe a singularity such as the negative compressibility which is observed for a system with two or three hard disks in a rectangular box [13,17,24]. We will comment on this in Sec. III.

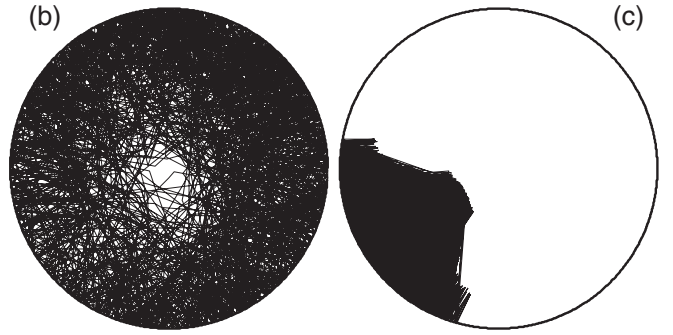
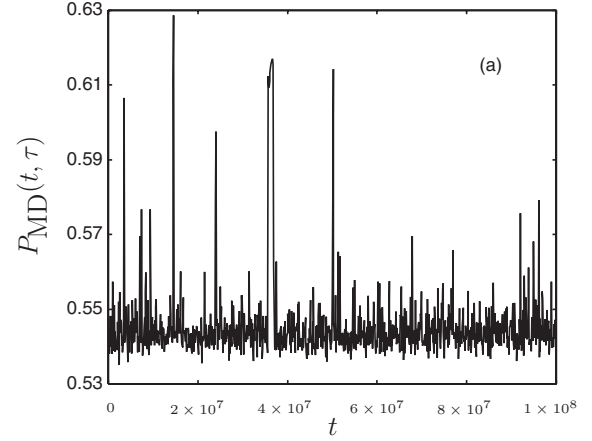


FIG. 3. (a) $P_{\text{MD}}(t, \tau)$ as a function of t . (b) Trajectory of \mathbf{q}_1 in the time interval between $t_1=3.5 \times 10^7$ and t_1+10^3 . (c) Trajectory of \mathbf{q}_1 in the time interval between $t_2=3.6 \times 10^7$ and t_2+10^3 . We set $R=1.5$, $\mathcal{E}=3/2$, and $\mathcal{L}=0$.

We observe in Fig. 2 that the statistical errors of the pressure for a system with small cavity size become somewhat large when $\mathcal{L}=0$. To focus on this point, we define $P_{\text{MD}}(t, \tau)$ by

$$P_{\text{MD}}(t, \tau) = \frac{1}{\tau} \frac{\sum_{i=1}^2 \sum_{n=1}^{N_{i,t}} 2p_{i,r}(n)}{2\pi R}, \quad (11)$$

where $N_{i,t}$ is the total number of collisions of the i th hard disk with the wall during the time from t to $t+\tau$. In Fig. 3(a), we show $P_{\text{MD}}(t, \tau)$ as a function of t for the case $R=1.5$, $\mathcal{E}=3/2$, and $\mathcal{L}=0$. Here we take $\tau=10^5$. $P_{\text{MD}}(t, \tau)$ mostly fluctuates between 0.54 and 0.55, i.e., around P predicted from Eq. (9), but sometimes it becomes large. In particular, $P_{\text{MD}}(t, \tau)$ continues to be larger than 0.6 for some duration of time around $t=3.6 \times 10^7$. This causes a large statistical error. To understand this behavior from the dynamics of hard disks, we show the trajectory $\mathbf{q}_1(t)$ in the time interval between $t_1=3.5 \times 10^7$ and t_1+10^3 in Fig. 3(b) with $P_{\text{MD}}(t_1, \tau)=0.542$. We also show $\mathbf{q}_1(t)$ in the time interval between $t_2=3.6 \times 10^7$ and t_2+10^3 in Fig. 3(c) with $P_{\text{MD}}(t_2, \tau)=0.611$. The disk can move in the whole circular cavity in the case of Fig. 3(b), while the trajectory in Fig. 3(c) is restricted to a part of the circular cavity. The second disk naturally behaves similarly.

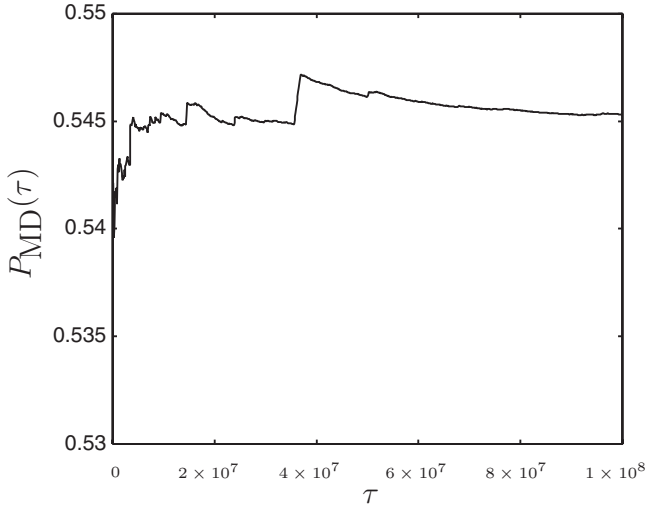


FIG. 4. $P_{\text{MD}}(\tau)$ as a function of τ for the same conditions as in Fig. 3.

Thus, this behavior is seen to come from the packing geometry. That is, when R is small and two hard disks are packed in a small space, the two hard disks form a kind of bound state with long lifetime. This quasinonergodic behavior recalls the real nonergodicity which was found for a rectangular box with two hard disks [13,17]. The pressure obtained from a molecular dynamics simulation deviates from the theoretical prediction when the system is in a bound state, since ergodicity of a system is a crucial factor for the validity of statistical mechanics.

To see the influence of this deviation on the pressure obtained from Eq. (10), we display $P_{\text{MD}}(\tau)$ as a function of τ in Fig. 4. We observe that $P_{\text{MD}}(\tau)$ relaxes toward the value computed from Eq. (9) even though it increases considerably around $t_2 = 3.6 \times 10^7$ for the reason noted above. Therefore, we believe that $P_{\text{MD}}(\tau)$ converges to P defined by Eq. (9) as $\tau \rightarrow \infty$.

Next our interest is in the dependence of pressure on \mathcal{L} . One may expect from Fig. 2 that the pressure decreases as $|\mathcal{L}|$ increases with total energy fixed. In Fig. 5, we plot the pressure as a function of the total angular momentum, and this plot shows the expected behavior. We take parameters in Fig. 5 that are the same as those in the case of the solid curve in Fig. 1.

We show in Fig. 6 the density $\rho(r)$ [Fig. 6(a)] and the mean radial energy $E_r(r)$ [Fig. 6(b)] at the distance r from the center of the cavity, which are defined by

$$\rho(r) = \frac{\left\langle \sum_{i=1}^2 \delta(r_i - r) \right\rangle}{2\pi r} \quad (12)$$

and

$$E_r(r) = \frac{1}{2\pi r \rho(r)} \left\langle \frac{\sum_{i=1}^2 p_{r,i}^2 \delta(r_i - r)}{2m} \right\rangle, \quad (13)$$

respectively. The density at the wall becomes large as $|\mathcal{L}|$ increases, which is interpreted as the effect of a centrifugal

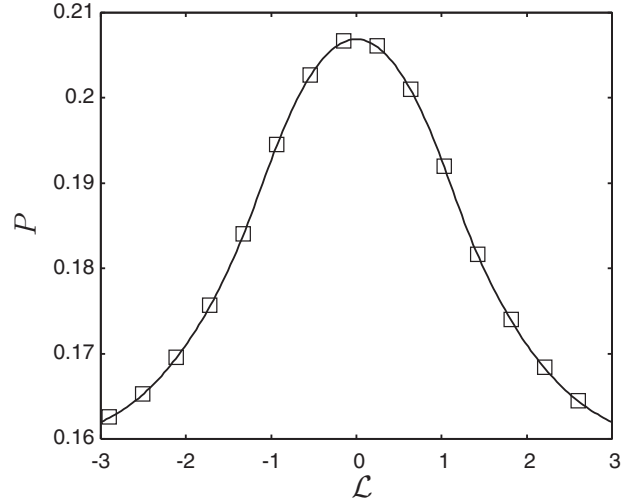


FIG. 5. Dependence of pressure on \mathcal{L} . Curve represents the result of Eq. (9). Points represent the result of molecular dynamics simulation. We set $\mathcal{E}=3/2$ and $R=2$.

force. The mean radial energy, which can be regarded as the temperature at r , is dependent on r except for $\mathcal{L}=0$, and is largest at the wall. This means that the average of the radial energy when a disk collides with the wall is larger than the temperature, because the temperature is interpreted as the average of the radial energy over the whole phase space volume. Position-dependent temperatures have been studied for other systems with conservation of the total angular momentum [25]. From Fig. 6, it is seen that the collision frequency with the wall increases, but the average force acting on the wall per collision decreases, as $|\mathcal{L}|$ increases.

III. TWO HARD SPHERES IN A CYLINDRICAL PORE

We turn to a system with two hard spheres in a cylindrical pore. Each hard sphere has a diameter d and mass m . The cylindrical pore has a radius R and a longitudinal length L . We can write the Hamiltonian of this system by using the position and the momentum of the i th hard sphere ($i=1,2$), which are denoted by $\mathbf{q}_i=(r_i, \theta_i, z_i)$ and $\mathbf{p}_i=(p_{r,i}, p_{\theta,i}, p_{z,i})$, respectively,

$$H_{\text{cyl}} = \sum_{i=1}^2 \left(\frac{p_{r,i}^2 + p_{z,i}^2}{2m} + \frac{p_{\theta,i}^2}{2mr_i^2} + V_{\text{ext}}(\mathbf{q}_i) \right) + V_{\text{int}}(|\mathbf{q}_1 - \mathbf{q}_2|), \quad (14)$$

where the expression for V_{int} is the same as Eq. (3), while V_{ext} is written as

$$V_{\text{ext}}(\mathbf{q}_i) = \begin{cases} 0, & 0 \leq r_i \leq R - d/2 \text{ and } d/2 \leq z_i \leq L - d/2, \\ \infty & \text{otherwise.} \end{cases} \quad (15)$$

Since this system also conserves the total energy \mathcal{E} and the z component of the total angular momentum \mathcal{L} , the phase space volume of this system, Γ_{cyl} , is obtained from a similar calculation as before [see Eq. (6)]

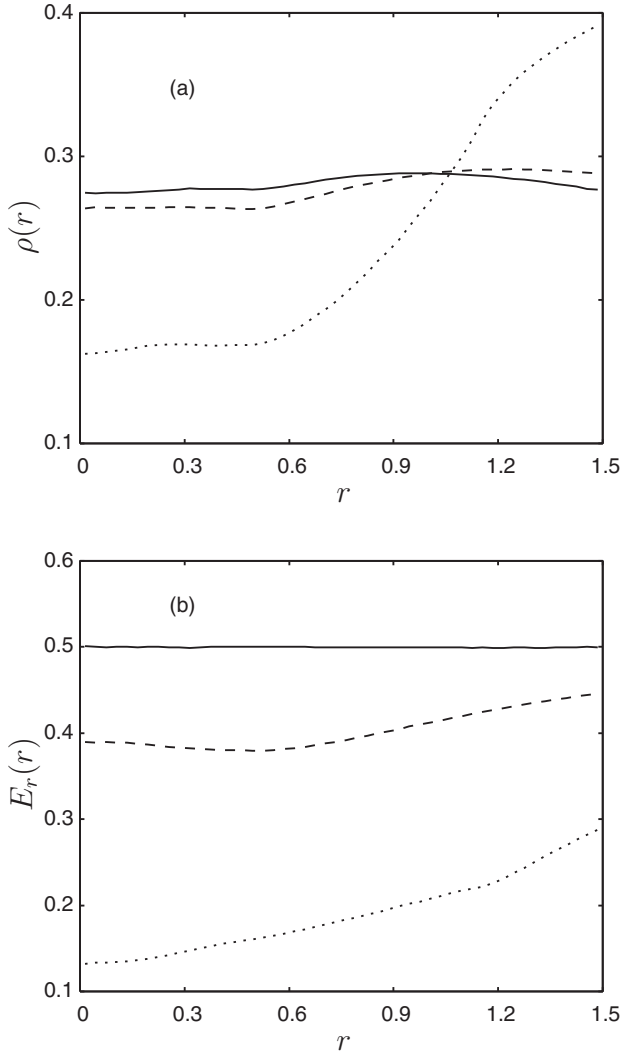


FIG. 6. (a) Density $\rho(r)$ defined by Eq. (12) and (b) mean radial energy $E_r(r)$ defined by Eq. (13) obtained from molecular dynamics simulations for $\mathcal{L}=0$ (solid curve), 1 (dashed curve), and 2 (dotted curve). We set $R=2$ and $\mathcal{E}=3/2$.

$$\begin{aligned} \Gamma_{\text{cyl}}(\mathcal{E}, \mathcal{L}) &= \int \left(\prod_{i=1}^2 dr_i d\theta_i dz_i dp_{r,i} dp_{\theta,i} dp_{z,i} \right) \Theta(\mathcal{E} - H_{\text{cyl}}) \\ &\times \delta \left(\mathcal{L} - \sum_{i=1}^2 p_{\theta,i} \right) \\ &\propto \int_0^{R-d/2} dr_1 \int_0^{R-d/2} dr_2 \int_0^{L-d} dz \frac{r_1 r_2 (L-d-z)}{(r_1^2 + r_2^2)^3} \\ &\times [2m\mathcal{E}(r_1^2 + r_2^2) - \mathcal{L}^2]^{5/2} h(r_1, r_2; z) \\ &\times \Theta(2m\mathcal{E}(r_1^2 + r_2^2) - \mathcal{L}^2) \end{aligned} \quad (16)$$

where $z=z_2-z_1$ and $h(r_1, r_2; z)$ is

$$h(r_1, r_2; z) = \begin{cases} g(r_1, r_2; \sqrt{d^2 - z^2}), & z \leq d, \\ 4\pi^2, & z > d, \end{cases} \quad (17)$$

with g defined by Eq. (7)

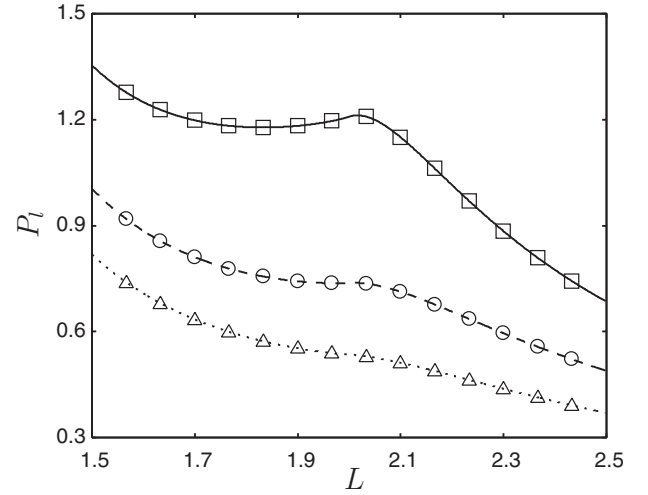


FIG. 7. P_l as a function of L for the system with two hard spheres in cylindrical pores with different R . Curves represent the result of Eq. (18) for $R=1.1$ (solid), 1.2 (dashed) and 1.3 (dotted). Points represent the result of simulations for $R=1.1$ (square), 1.2 (circle), and 1.3 (triangle). We set $\mathcal{L}=0$ and $\mathcal{E}=5/2$.

We define the entropy of this system by $S = \ln \Gamma_{\text{cyl}}(\mathcal{E}, \mathcal{L})$ and other thermodynamic quantities are obtained from S [18,19,23], e.g., the pressures in the longitudinal and the radial direction, denoted by P_l and P_r , respectively, are given by

$$P_l = \frac{T}{\pi R^2} \left(\frac{\partial S}{\partial L} \right), \quad (18)$$

$$P_r = \frac{T}{2\pi RL} \left(\frac{\partial S}{\partial R} \right), \quad (19)$$

where T is defined by Eq. (8). Hereafter our attention is paid to the pressure P_l because the behaviors of the temperature and pressure in the radial direction for this system resemble those for the system of two hard disks in a circular cavity. In Fig. 7, we consider the dependence of P_l on the size of the cylindrical pore. We depict $P_l = P_l(L, R, \mathcal{E}, \mathcal{L})$ as a function of L in Fig. 7. As in Sec. II, we choose m and d as the units of mass and length, and we set $\mathcal{E}=5/2$ and $\mathcal{L}=0$. It is seen from Fig. 7 that a negative compressibility region, i.e., a region where the pressure increases as L increases, exists around $L=2$, when $R=1.1$, but this region disappears when R becomes large.

The reason for the occurrence of negative compressibility is explained as follows. P_l increases monotonically when L decreases from $L=2.5d$, because the volume of the pore decreases. As L approaches $2d$, a configuration in which two spheres have considerable contact with each other along the z axis produces pressure on the surfaces. This configuration gives higher pressure compared with other configurations, and this effect is large for small R . If L further decreases from $L \approx 2d$, then the probability of this configuration decreases drastically. This causes a decrease of pressure when L decreases around $L \approx 2d$. When L decreases further, P_l increases again because of reduction of the size of the pore.

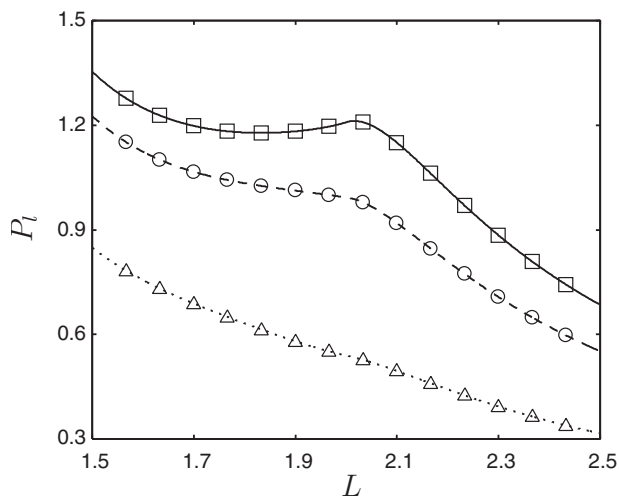


FIG. 8. P_l as a function of L for the system with two hard spheres in cylindrical pores with different \mathcal{L} . Curves represent the result of Eq. (18) for $\mathcal{L}=0$ (solid), 0.5 (dashed), and 1 (dotted). Points represent the result of simulations for $\mathcal{L}=0$ (squares), 0.5 (circles), and 1 (triangles). We set $R=1.1$ and $\mathcal{E}=5/2$.

As a result, the negative compressibility region appears when R is relatively small. On the other hand, for the system discussed in Sec. II, the phenomenon mentioned above does not occur because of the shape of the cavity.

Next we discuss the L and \mathcal{L} dependence of P_l . In Fig. 8, we depict P_l as a function of L for $\mathcal{L}=0, 0.5$, and 1. The other conditions are the same for the three curves. We can see from Fig. 8 that the compressibility is negative around $L=2$ when $\mathcal{L}=0$, while the compressibility is always positive for $\mathcal{L}=0.5$ and 1.

Now, we consider P_l as a function of L, R, T , and \mathcal{L} , i.e., $P_l=P_l(L,R,T,\mathcal{L})$, instead of $P_l=P_l(L,R,\mathcal{E},\mathcal{L})$. Then \mathcal{E} has to be adjusted in order to obtain a T specified in advance. In Fig. 9, we depict P_l as a function of L for $\mathcal{L}=0, 0.5$, and 1 with $R=1.1$ and $T=1$. The negative compressibility region is still observed when $\mathcal{L}=0$ and this region disappears when \mathcal{L} becomes large. The difference in P_l among the three curves in Fig. 9 turns out to be small as compared with the three curves in Fig. 8. This is because \mathcal{E} has to increase to keep the temperature constant when \mathcal{L} increases.

IV. SUMMARY

In summary, we have investigated systems consisting of two hard disks in a circular cavity and two hard spheres in a cylindrical pore by using statistical mechanics and molecular dynamics simulations. We adopted these vessels to confine the particles and to satisfy conservation of both the total energy \mathcal{E} and the total angular momentum \mathcal{L} . It is noted that the phase space volume Eq. (5) played a fundamental role in the theoretical approach.

At this point, we comment on some recent works which also deal with the conservation of the total angular momentum in addition to the total energy, based on similar methods [26–30]. The systems studied there are composed of particles with attractive interaction, e.g., self-gravitating and Lennard-

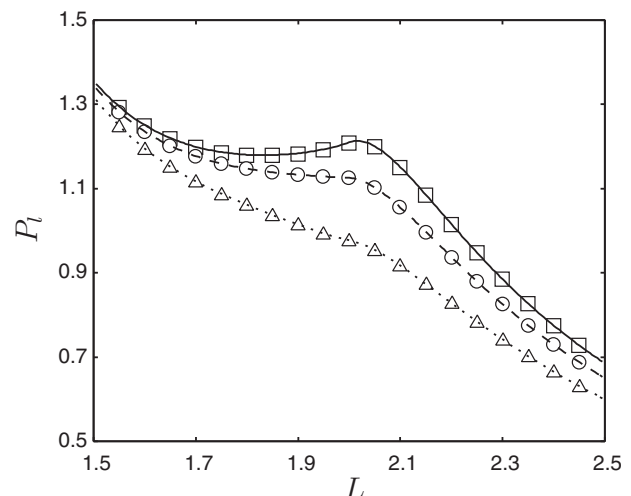


FIG. 9. P_l as a function of L for the system with two hard spheres in cylindrical pores with the same T and different \mathcal{L} . Curves represent the result of Eq. (18) for $\mathcal{L}=0$ (solid), 0.5 (dashed), and 1 (dotted). Points represent the result of simulations for $\mathcal{L}=0$ (squares), 0.5 (circles), and 1 (triangles). We set $R=1.1$ and $T=1$, and \mathcal{E} is adjusted to realize $T=1$.

Jones systems, and the particles need not be put in a vessel. For most of these investigations, the Dirac δ function is used in the definition of the phase space volume, while we used the Heaviside function in Eq. (5). For systems with many degrees of freedom, the difference between the two definitions of the phase space volume is not important [31]. However, for small systems, this difference may be important, and we confirmed in this paper that our numerical results are actually supported by the definition Eq. (5).

Our first subject of interest is the dependence of thermodynamic quantities such as temperature T , Eq. (8), and pressure P , Eq. (9), on both \mathcal{E} and \mathcal{L} . In the theoretical approach, we computed the phase space volume, Eq. (5), and obtained the temperature and pressure from the entropy [18–21], which is related to the phase space volume through the thermodynamic relation Eq. (4). In general, it is found that the pressure decreases as $|\mathcal{L}|$ increases with the size of the vessel kept constant.

In addition to the \mathcal{L} dependence of thermodynamic quantities, we have also discussed the nonergodic behavior of the system with two hard disks in a circular cavity, which was discovered in the process of analyzing large fluctuations of the pressure. We found that the motion of hard disks is sometimes restricted to a small part of a cavity for a long time, when the size of the cavity and the total angular momentum are small. One encounters a similar situation when one observes the dynamics of other Hamiltonian systems [32]. From this and the real nonergodic transition for two hard spheres(disks) in rectangular boxes, we expect interesting nonergodic behavior for highly compressed systems.

ACKNOWLEDGMENTS

The author thanks Professor T. Munakata for useful discussions.

- [1] L. D. Gelb, K. E. Gubbins, R. Radhakrishnan, and M. Sliwiska-Bartkowiak, *Rep. Prog. Phys.* **62**, 1573 (1999).
- [2] C. Alba-Simionesco, B. Coasne, G. Dosseh, G. Dudziak, K. E. Gubbins, R. Radhakrishnan, and M. Sliwiska-Bartkowiak, *J. Phys.: Condens. Matter* **18**, R15 (2006).
- [3] Z. T. Németh and H. Löwen, *J. Phys.: Condens. Matter* **10**, 6189 (1998).
- [4] Z. T. Németh and H. Löwen, *Phys. Rev. E* **59**, 6824 (1999).
- [5] F. L. Román, A. González, J. A. White, and S. Velasco, *J. Chem. Phys.* **118**, 7930 (2003).
- [6] F. L. Román, A. González, J. A. White, and S. Velasco, *Physica A* **334**, 312 (2004).
- [7] I. E. Kamenetskiy, K. K. Mon, and J. K. Percus, *J. Chem. Phys.* **121**, 7355 (2004).
- [8] D. A. Kofke and A. J. Post, *J. Chem. Phys.* **98**, 4853 (1993).
- [9] T. Taniguchi and G. P. Morriss, *Phys. Rev. E* **68**, 026218 (2003).
- [10] T. Taniguchi and G. P. Morriss, *Phys. Rev. Lett.* **94**, 154101 (2005).
- [11] G. T. Pickett, M. Gross, and H. Okuyama, *Phys. Rev. Lett.* **85**, 3652 (2000).
- [12] M. C. Gordillo, B. Martínez-Haya, and J. M. Romero-Enrique, *J. Chem. Phys.* **125**, 144702 (2006).
- [13] T. Munakata and G. Hu, *Phys. Rev. E* **65**, 066104 (2002).
- [14] M. Uranagase and T. Munakata, *Phys. Rev. E* **74**, 066101 (2006).
- [15] R. J. Speedy, *Physica A* **210**, 341 (1994).
- [16] I. H. Umirzakov, *Phys. Rev. E* **61**, 7188 (2000).
- [17] A. Awazu, *Phys. Rev. E* **63**, 032102 (2001).
- [18] V. L. Berdichevsky, *Thermodynamics of Chaos and Order* (Addison-Wesley/Longman, London, 1997).
- [19] V. L. Berdichevskii, *J. Appl. Math. Mech.* **52**, 738 (1988).
- [20] V. L. Berdichevsky and M. v. Alberti, *Phys. Rev. A* **44**, 858 (1991).
- [21] V. M. Bannur, P. K. Kaw, and J. C. Parikh, *Phys. Rev. E* **55**, 2525 (1997).
- [22] A. B. Adib, *J. Stat. Phys.* **117**, 581 (2004).
- [23] H. H. Rugh, *Phys. Rev. E* **64**, 055101(R) (2001).
- [24] Z. Cao, H. Li, T. Munakata, D. He, and G. Hu, *Physica A* **334**, 187 (2004).
- [25] T. Niiyama, Y. Shimizu, T. R. Kobayashi, T. Okushima, and K. S. Ikeda, *Phys. Rev. Lett.* **99**, 014102 (2007).
- [26] R. S. Dumont, *J. Chem. Phys.* **95**, 9172 (1991).
- [27] S. C. Smith, *J. Chem. Phys.* **97**, 2406 (1992).
- [28] F. Calvo and P. Labastie, *Eur. Phys. J. D* **3**, 229 (1998).
- [29] V. Laliena, *Phys. Rev. E* **59**, 4786 (1999).
- [30] O. Fliegans and D. H. E. Gross, *Phys. Rev. E* **65**, 046143 (2002).
- [31] M. Toda, R. Kubo, and N. Saito, *Statistical Physics I: Equilibrium statistical mechanics* (Springer-Verlag, Berlin, 1992).
- [32] G. M. Zaslavsky, *Phys. Rep.* **371**, 461 (2002).